

Multi-Objective Path Planning of an Autonomous Mobile Robot in Static and Dynamic Environments using a Hybrid PSO-MFB Optimisation Algorithm

Ibraheem Kasim Ibraheem ^{1*}, Fatin Hassan Ajeil ²

^{1,2}Electrical Engineering Department, College of Engineering, University of Baghdad, 10001, Baghdad, Iraq

* Ibraheemki@coeng.uobaghdad.edu.iq

Abstract: The main aim of this paper is to solve a path planning problem for an autonomous mobile robot in static and dynamic environments by determining the collision-free path that satisfies the chosen criteria for shortest distance and path smoothness. The algorithm mimics the real world by adding the actual size of the mobile robot to that of the obstacles and formulating the problem as a moving point in the free-space. The proposed path planning algorithm consists of three modules: in the first module, the path planning algorithm forms an optimised path by conducting a hybridized Particle Swarm Optimization-Modified Frequency Bat (PSO-MFB) algorithm that minimises distance and follows path smoothness criteria; in the second module, any infeasible points generated by the proposed PSO-MFB Algorithm are detected by a novel Local Search (LS) algorithm and integrated with the PSO-MFB algorithm to be converted into feasible solutions; the third module features obstacle detection and avoidance (ODA), which is triggered when the mobile robot detects obstacles within its sensing region, allowing it to avoid collision with obstacles. Simulations have been carried out that indicated that this method generates a feasible path even in complex dynamic environments and thus overcomes the shortcomings of conventional approaches such as grid methods. Comparisons with previous examples in the literature are also included in the results.

1. Introduction

Autonomous navigation of mobile robots cover a wide spectrum of applications, including restaurants [1], libraries, and industrial and rescue robots [2]. The success of mobile robots in these applications depend on their intelligence capabilities, and of these capabilities, *path planning* is one of the most effective and important. This involves the creation of an optimised collision-free path from one place to another. Path planning can be divided into various categories depending on the nature of the environment: *static path planning*, where obstacles do not change their position with time, and *dynamic path planning* where the position and orientation of obstacles change with time. These can be further subdivided according to the knowledge level of the mobile robot into *offline* and *online* algorithms. In *offline* path planning, the mobile robot has a complete knowledge of the environment. Consequently, the path planning algorithm produces a complete path before mobile robot begins motion. In *online* path planning, however, information about the environment is obtained from a local sensor attached to the mobile robot, and the mobile robot requires the ability to construct a new path in response to the changes in the environment. This categorisation can be further subcategorised according to the target nature, into *stationary target*, where the mobile robot is searching for a static point in its workspace, and once it has located this point, never moves away from it; and *dynamic target*, wherein the mobile robot must search for a moving target while avoiding obstacles. In the latter case, the mobile robot and its target are both in motion [3]. Each scenario requires different path planning algorithms, and combinations of one or more of the aforementioned situations may require particularly complicated path planning algorithms.

Path planning studies began in the late 1960s, and various techniques have been suggested involving cell

decomposition [4], roadmap approaches [5], and potential fields [6]. The main drawbacks of these algorithms are inefficiency, because of high computational costs, and inaccuracy, because of the high risk of getting stuck in local minima. Adopting various heuristic methodologies can defeat the impediments of these algorithms, and these include the application of neural systems, genetics, and nature-inspired algorithms [7]. Rapid satisfactory solutions are one of the leading significant focal points of such heuristic methodologies, and these are particularly appropriate for finding solutions to NP-complete problems.

The current paper is structured as follows. First, section 2 highlights several research methodologies, then section 3 presents the problem statement, preliminaries, and the performance criteria considered in this work. Swarm based optimization is introduced in section 4, while in section 5, the methodologies proposed for mobile robot path planning in this work are introduced. In section 6, a set of simulation results are presented to demonstrate the effectiveness of the proposed methodology as compared with previous work. Finally, this paper concludes in section 7 with recommendations for future work.

2. Related Works

The primary requirement of autonomous mobile robots is to optimise the collision-free paths used. Numerous approaches have been used to solve single/multi-objective path planning problems for mobile robots, such as swarm/nature-inspired algorithms, neural networks, and fuzzy logic. The first group includes several previous studies that have exploited examples of natural swarm behaviours. The work in [8] utilised the standard Ant Colony optimization (ACO) to solve path planning problems for complex environments. The modified version of ACO exploiting the age of the ants proposed in [9] has been applied to path planning using a grid-based method.

Numerous works have also adopted heuristic methods and employed these to solve different aspects of path planning heuristic methods such as Particle Swarm Optimisation [8, 9], Cuckoo search (CS) algorithms [10], Self-adaptive bacterial foraging optimisation (SABFO) [11], Artificial Immune Systems [12], and the Whale Optimisation Algorithm (WOA), which was implemented in a static environment to satisfy requirements for the shortest and smoothest path in [13]. GA and its modified versions are frequently implemented to find the shortest path for mobile robot path planning in different environments [14–16], while path planning using neural networks was developed in [17–20]. Integrating a path planning algorithm with the motion controllers of mobile robots was achieved in [21–25], where several different motion control strategies were employed, including fuzzy logic controls, adaptive neuro-fuzzy inference systems, and model predictive controls. The Wind Driven Optimisation (WDO) and Invasive Weed Optimisation (IWO) algorithms were used to tune the parameters of the fuzzy logic controller and adaptive neuro-fuzzy inference systems in [22, 23], respectively, while ACO and PSO were used in the tuning of the fuzzy logic controller presented by [24]. The works in [26–28] incorporated two-level navigation algorithms, where the higher level was mainly concerned with path planning and guidance for the mobile robot, while the motion control directing the mobile robot in its configuration space was included in the lowest level. Path planning with energy constrained objective measures were demonstrated in [29, 30]. The work in [7], and the references therein, are noted as a particularly excellent survey for path planning problems in mobile robots.

One of the drawbacks in the studies mentioned is that throughout, the mobile robot was treated as a simple particle. While some of these algorithms were oriented toward finding the shortest path while avoiding static obstacles, others focused on the avoidance of dynamic obstacles while achieving the shortest distance without considering the smoothness of the path. Moreover, despite the ease of implementation of the grid-based methods used by some of the above researches, these have several disadvantages such as the imprecise representation of the obstacle, where if the obstacle occupies only a small area of the cell, the entire cell is nevertheless reserved for that obstacle. This leads to the waste of a space and less flexibility in a dynamic environment.

Paper Contribution. The contribution of this paper is the development of a new path planning algorithm which consists of three main modules: the first module involves *point generation*, achieved using a novel heuristic nature-inspired algorithm, which is a hybridization between Particle Swarm Optimization and Modified Frequency Bat Algorithms, thus a PSO-MFB Algorithm. This fused algorithm generates and select the points that satisfy the multi-objective measure proposed in this work, which is a combination of shortest path and path smoothness. This algorithm was integrated with a second module, the *Local Search* technique, which converts infeasible solutions into feasible ones. In addition, to avoid obstacles, twelve sensors are deployed around the mobile robot to sense obstacles, and once such are detected, an avoidance algorithm is triggered. This is achieved in the third module, the *Obstacle avoidance* module. To the best of the authors' knowledge, no study found in the literature has previously combined a heuristic

optimisation algorithm, Local Search technique, and obstacle avoidance in a single integrated path planning algorithm.

3. Problem Statement and Preliminaries

Assume a mobile robot at a start position (SP) that is required to reach a goal position (GP); several static and dynamic obstacles are also assumed to exist in the mobile robot workspace. The objective of a path planning problem is to find an optimum or near-optimum path (safest, shortest, and smoothest) without colliding with any of the obstacles in the workspace. Before discussing and suggesting solutions to this problem, some of the assumptions made in this paper should be made explicit.

Assumption 1: The obstacles are represented as circular shapes.

Assumption 2: The mobile robot is a physical body; thus, to take into account the actual size of the mobile robot, the obstacles are expanded by the radius of mobile robot (r_{MR}), so that the mobile robot can be considered as a point, as shown in Fig. 1.

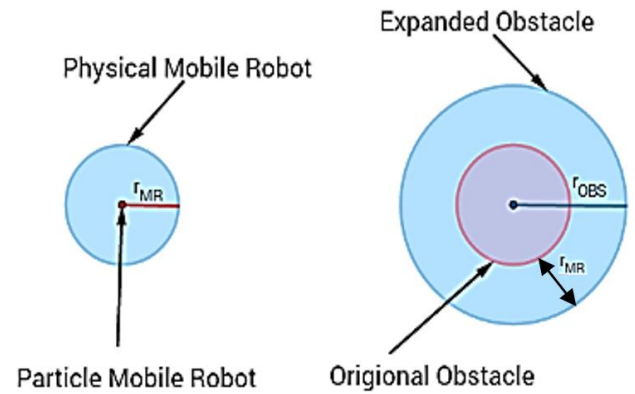


Fig. 1. Expanding obstacles size corresponding to mobile robot size.

Assumption 3: There are no kinematic constraints which affect the motion of the mobile robot. The only effective source is the motion of the obstacles.

Assumption 4: The mobile robot motion is omnidirectional, and the mobile robot can move in any direction at any time.

3.1. The Performance Criteria

1. Shortest Distance: In the path planning field, this means minimising the path length between the start and goal points. The total path length is the sum of all distances between mid-points ($wp_j(1), \dots, wp_j(N)$) generated by the path planning algorithm between this Start Point (SP) $wp_j(0)$ and the Goal Point (GP) $wp_j(N + 1)$, as shown:

$$f_1(x, y) = d(wp_j(t), wp_i(t + 1)) = \sum_{t=0}^N d_t \quad (1)$$

where,

$$d_t = \sqrt{(x_{wp_i(t+1)} - x_{wp_j(t)})^2 + (y_{wp_i(t+1)} - y_{wp_j(t)})^2}$$

2. Path Smoothness: This involves minimising the difference of the angles between the straight lines (goal-current points and suggested points-current point), as shown in Fig. 2.

This is given by

$$f_2(x, y) = \sum_{i=0}^N |\theta_{(i,i+1)} - \theta_{(i,N+1)}| \quad (2)$$

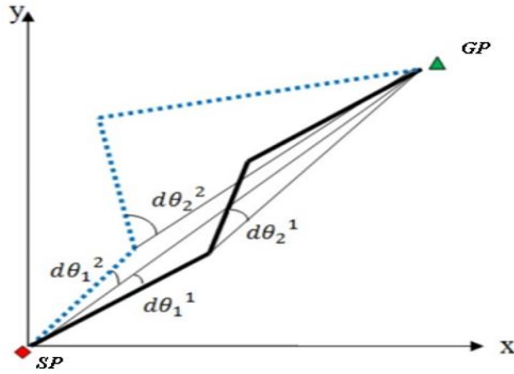


Fig. 2. Path smoothness: Summing Angles errors.

$$\text{where } \theta_{(i,i+1)} = \tan^{-1} \frac{y_{i+1}-y_i}{x_{i+1}-x_i}, \theta_{(i,N+1)} = \tan^{-1} \frac{y_{N+1}-y_i}{x_{N+1}-x_i}$$

The overall multi-objective optimization is the weighted sum of the above two objectives:

$$f(x, y) = w_1 f_1(x, y) + w_2 f_2(x, y) \quad (3)$$

where w_1 and w_2 are degrees of importance of the two objectives. Their values must satisfy the following constraints:

$$w_1 + w_2 = 1 \quad (4)$$

$$\text{fitness} = \frac{1}{f(x, y) + \varepsilon} \quad (5)$$

where ε is small number (e.g., $\varepsilon = 0.001$). The process of selecting the best solution among competing feasible options in each iteration depends on the balance between the two performance objectives declared in (1) and (2) for all available solutions. In Fig. 3, the best point among six competing points is point wp_3 for the t -th iteration, and point wp_5 in $(t+1)$ -th iteration, while in the $(t+2)$ -th iteration, points wp_2 and wp_3 offer shorter distances but larger difference angles, in contrast to point wp_1 which provides a balance between the two criteria; thus, point wp_1 is selected. This process is continued until reaching GP.

3.2. Obstacles Movement

In each time step, the obstacle changes its location continuously. In this work, the movement of the dynamic obstacles are considered to be one of the following types:

A. Linear movement

In this case, the obstacles move in a straight line with specific velocity (v_{obs}) and direction (φ_{obs}) according to the following relationship:

$$x_{obs_New} = x_{obs} + v_{obs} \times \cos \varphi_{obs} \quad (6)$$

$$y_{obs_New} = y_{obs} + v_{obs} \times \sin \varphi_{obs} \quad (7)$$

where φ_{obs} is the slope of the linear motion.

B. Circular trajectory

The obstacles move along circular path given by the centre of the circle (x_c, y_c) and the radius (r_c). Thus, the new position of the obstacle is given by:

$$x_{obs} = x_c + r_c \times \cos \theta \quad (8)$$

$$y_{obs} = y_c + r_c \times \sin \theta \quad (9)$$

The range of θ represents the portion of circular arc for complete circle ($0 < \theta < 2\pi$).

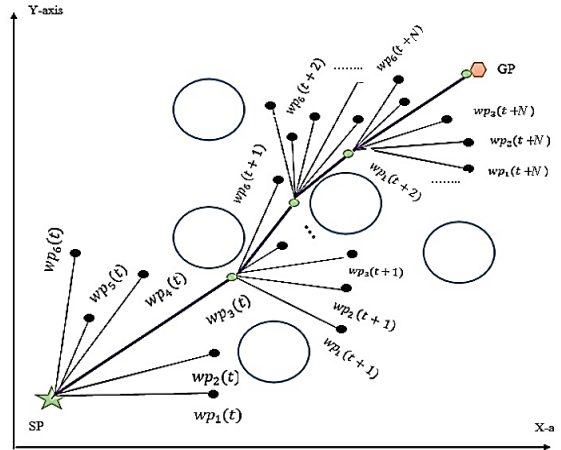


Fig.3. Mid-points selection for multi-objective path planning.

4. Swarm-based Optimization

Swarm Intelligence (SI) is an artificial collection of simple agents based on nature-inspired behaviours that can be successfully applied to optimisation problems in a variety of applications. The search process of such optimisation algorithms continues to find new solutions until the stopping criteria are satisfied (either the optimal solution is found, or a maximum number of iterations is reached). These SI behaviours can be used to solve a variety of problems, and thus there are several SI-based algorithms. Two such algorithms are used in this paper.

4.1. Particle Swarm Optimization (PSO) Algorithm

This is a population-based heuristic strategy for optimisation problems developed by J. Kennedy and R. C. Eberhard in 1995 [31], stimulated by the social conduct of schooling fish and flocking birds. It consists of a swarm of particles, and each particle in PSO has a position x_i and velocity v_i . The position represents a solution suggested by the particle, while the velocity is the rate of change to the next position with respect to the current position. These two values (position and velocity) are randomly initialized, and the solution construction of a PSO algorithm includes two phases, as shown below:

• Velocity Update of the Particle

$$v_i(t+1) = v_i(t) + c_1 r_1 (pbest_i - x_i) + c_2 r_2 (gbest - x_i) \quad (10)$$

• Position Update of the Particle

$$x_i(t+1) = x_i(t) + v_i(t+1) \quad (11)$$

From (10), the velocity of the particle i is affected by three main components: the particle's old velocity $v_i(t)$; a linear attraction toward the personal best position ever found ($pbest_i - x_i$), scaled by the weight c_1 and a random number $r_1 \in [0, 1]$; and the final component is a linear attraction towards the global best position found by any particle in the swarm ($gbest - x_i$), scaled by weight c_2 and a random number $r_2 \in [0, 1]$. The position of particles for $t+1$ -th iterations is updated according to (11).

4.2. Modified Frequency Bat (MFB) Algorithm

The Bat Algorithm (BA) is a bio-inspired algorithm developed by Yang in 2010 [32]. It is based on the echolocation or bio-sonar characteristics of micro bats.

Echolocation is an important feature of bat behaviour: the bats emit sound pulses and listen to the echoes bouncing back from obstacles while flying. By utilising the time difference between its ears, the loudness of the response, and the delay time, a bat can thus figure out the velocity, shape, and size of prey and obstacles. A bat also has the ability to change the way its sonar works. If it sends sound pulses at a high rate, it can fly for less time while obtaining thorough details about its surroundings.

4.2.1. The Movement of Artificial Bats

The updating process of bat positioning is as follows:

$$f_i = f_{min} + (f_{max} - f_{min}) * \beta_i \quad (12)$$

$$v_i(t+1) = v_i(t) + (x_i(t) - x^*)f_i \quad (13)$$

$$x_i(t+1) = x_i(t) + v_i(t+1) \quad (14)$$

where β is a random number that increases with time for each bat generating low frequencies at the early stages of the search process. These frequencies increase with time to improve the global search performance [33], where x^* is the present global best location solution, found after making a comparison between all the solutions among all m bats. For the local search stage, once a solution is selected among the current best solutions, a new solution is generated for each bat locally using random walk:

$$x_{new} = x_{old} + \sigma \epsilon A(t) \quad (15)$$

where $\epsilon \in [-1, 1]$ is a random number, $A(t)$ is the average loudness of all the bats at time step t , and σ is a scaling parameter included to control the step size.

4.2.2. Loudness and Pulse Emission

The loudness, A_i , and the rate of pulse emission, r_i , must be updated as the iterations proceed. The loudness usually decreases once a bat has found its prey, whereas the rate of pulse emission increases according to the following equations:

$$A_i(t+1) = \alpha A_i(t) \quad (16)$$

$$r_i(t+1) = r_i(0)[1 - \exp(-\gamma t)] \quad (17)$$

where $0 < \alpha < 1$ and $\gamma > 0$ are design parameters.

5. Main Results

This section describes the proposed path planning algorithm for a mobile robot with omnidirectional motion based on hybridized swarm optimisation integrated with Local Search and obstacle avoidance techniques.

5.1. Proposed Hybrid PSO-MFB Algorithm

Hybridisation refers to mixing two or more optimisation algorithms to obtain the advantages of all of these algorithms, and thus, as a result, increasing the overall performance of the optimisation process. In this paper, a hybridisation between PSO and MFB algorithms is proposed. The variations of loudness, A_i , and pulse emission rates, r_i , also provide an auto zooming capability for the optimisation algorithm. Finding the optimum values of the MFB algorithm parameters (α, γ) is handled by the PSO algorithm. However, such parameter settings may be problem-dependent and thus tricky to define. In addition, the use of time-varying parameters during such iterations may be advantageous. The

proper control of such parameters can thus be important, and consequently, variations of the parameter α (hence the loudness A_i) and the parameter γ (hence the pulse rate r_i) within a suitable range have been adapted by the PSO algorithm to find a balance between *exploration* and *exploitation* in the MFB algorithm. The pseudo code for the proposed Hybrid PSO-MFB algorithm is shown in **Algorithm 1** and the overall procedure of the proposed Hybrid PSO-MFB algorithm is shown in Fig 4.

Algorithm 1: Pseudo code for Proposed Hybrid PSO-MFB

Step 1: Initialize PSO and MFB parameters: population size of n particles, r_1, r_2, c_1, c_2 , population size of m bats, frequencies f_i , pulse rates r_i and the loudness A_i .

Step 2: Randomly generate an initial solutions, $x_1 = [\alpha_1, \gamma_1]$, $x_2 = [\alpha_2, \gamma_2]$, ..., $x_n = [\alpha_n, \gamma_n]$.

Step 3: for $i = 1: n$

 Call MFB algorithm, (12)-(17)

end

- Choose the best bat that achieves the best fitness defined in (5), e.g. x_{kj} , $j=1:m$.
- Store index (k).
- $Gbest = x_k = [\alpha_k, \gamma_k]$

Step 4: If stopping criteria not satisfied

- Update velocity and position of particles according to (10)-(11).
- Go to step 2.

else

 obtain results

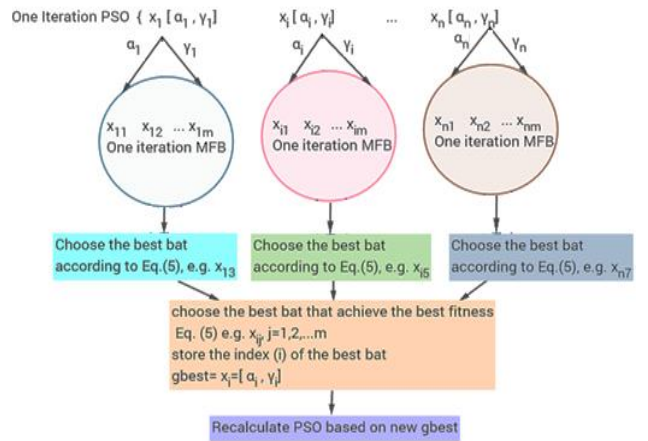


Fig. 4. Proposed Hybrid PSO-MFB algorithm.

The solution of the PSO in the proposed algorithm is a vector of dimension 2, where $x(1,1)$ represents the value of α while $x(1,2)$ is the value of γ .

5.2. Proposed Local Search (LS) Technique

The solution is considered infeasible if the next point generated by the hybrid PSO-MFB algorithm lies within an area occupied by an obstacle. Another infeasible solution is where the next point, $wp_j(t+1)$, forms a line segment with the previous point, $wp_j(t)$, and this line passes through the obstacle.

The *LS* technique converts these infeasible solutions into feasible ones. These two situations are explained in the following section with the aid of graphical and mathematical illustrations of the proposed solutions.

5.2.1. The points lie inside the obstacle

This situation is shown in Fig. 5 (a). It is checked by computing the Euclidean distance $d(wp_j(t), P_{obs})$ using (1) between the candidate point, $wp_j(t)$, and the centre of the obstacle $P_{obs} = (x_{obs}, y_{obs})$. If $d(wp_j(t), P_{obs})$, or simply d , is less than the obstacle's radius, r_{OBS} , then it is considered an infeasible candidate solution:

$$d(wp_j(t), P_{obs}) < r_{OBS} \quad (18)$$

This case is resolved by ousting these candidate solutions outside the area occupied by the obstacle according to the following suggested rules; see Fig. 5(b):

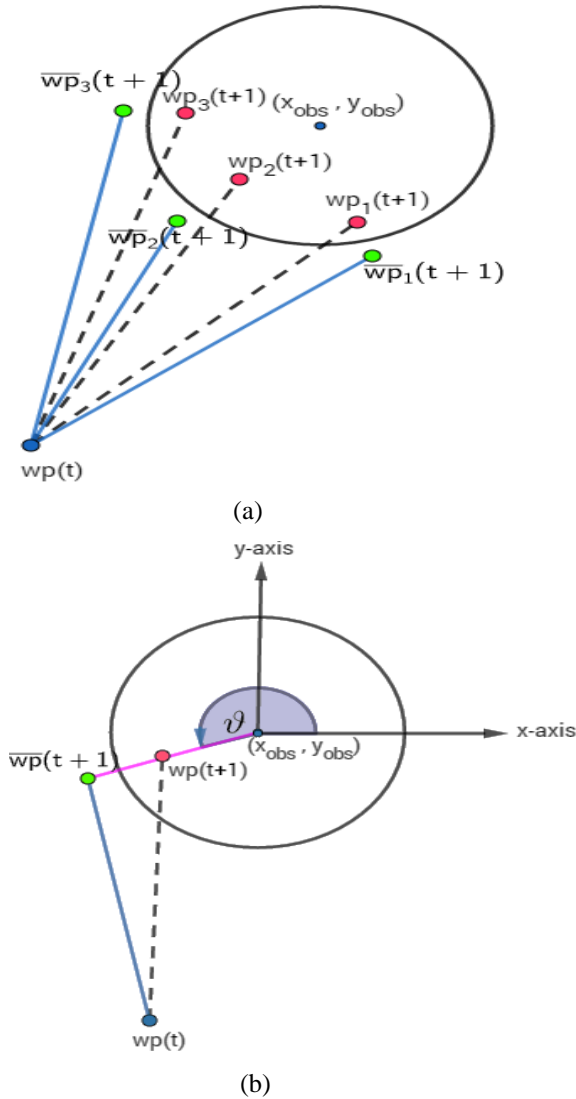


Fig. 5. Infeasible path types: the point lie inside the obstacle.

$$\bar{x}_{wp_j(t+1)} = x_{wp_j(t+1)} + (r_{OBS} + ds - d) \times \cos \vartheta_j \quad (19)$$

$$\bar{y}_{wp_j(t+1)} = y_{wp_j(t+1)} + (r_{OBS} + ds - d) \times \sin \vartheta_j \quad (20)$$

where ds refers to the minimum safety distance (say $ds = 0.2$), ϑ_j is the angle between obstacle centre, and j -th is candidate point $wp_j(t)$. Therefore, the red points in Fig. 5

represent the candidate solutions generated by the hybrid PSO-MFB Algorithm, while the green ones are the updated ones according to (19) and (20), where $\bar{wp}(t+1) = (\bar{x}_{wp_j(t)}, \bar{y}_{wp_j(t)})$. This proposed Local Search scenario is illustrated in example (1).

Example (1): Suppose that the obstacle position $obs_{pos} = (2, 3)$, radius of the obstacle $r_{OBS} = 1$, and the candidate point suggested by hybrid PSO-MFB Algorithm is $wp(t+1) = (1.7, 2.4)$.

check: Calculate the distance between P_{obs} & wp :

$$d = \sqrt{(x_{obs} - x_{wp(t+1)})^2 + (y_{obs} - y_{wp(t+1)})^2}$$

$$d = \sqrt{(2 - 1.7)^2 + (3 - 2.4)^2} = 0.6708$$

The condition in (18) is true, i.e., $d < r_{OBS}$. This means that the candidate point lies inside the obstacle region.

Solution:

$$\vartheta = 180 + \tan^{-1} \frac{y_{obs} - y_{wp(t+1)}}{x_{obs} - x_{wp(t+1)}}$$

$$\vartheta = 180 + \tan^{-1} \frac{3 - 2.4}{2 - 1.7} = 180^\circ + 63.4^\circ$$

Using (19) and (20), the corrected solution is $\bar{x}_{wp_j(t+1)} = x_{wp} + (1 + 0.2 - 0.6708) \times \cos \vartheta = 1.4$

$$\bar{y}_{wp_j(t+1)} = y_{wp} + (1 + 0.2 - 0.6708) \times \sin \vartheta = 1.9$$

$$\bar{wp}(t+1) = (\bar{x}_{wp_j(t+1)}, \bar{y}_{wp_j(t+1)}) = (1.4, 1.9).$$

5.2.2. The line segment passes through the obstacle

The second situation is shown in Fig. 6 (a); here, a line segment that connects two consecutive points, $wp_j(t)$ and $wp_j(t+1)$, passes through the region occupied by the obstacle. This situation can be resolved using the following procedure:

1. Find the equation of the line segment that connects any two consecutive points as shown in Fig. 6 (b).

$$y = mx + c \quad (21)$$

Substitute y as given by (21) into the circle equation that describes the obstacle circumference:

$$(x - x_{obs})^2 + (y - y_{obs})^2 = (r_{OBS})^2 \quad (22)$$

2. Solve for x to find whether the line intersects with the obstacle. The resulting equation will be quadratic and in terms of only x , and its solution is given as

$$x_{1,2} = \frac{-b \pm \sqrt{b^2 - 4ac}}{2a} \quad (23)$$

The exact behaviour depends on $b^2 - 4ac$ and is determined by the three possible solutions:

- if $b^2 - 4ac < 0$, then $x_{1,2}$ are complex. Here, the path segment does not intersect with the obstacle and the path is a *feasible solution*.
- if $b^2 - 4ac = 0$, then $x_{1,2}$ has a single solution. The path segment is tangential to the obstacle and the path is considered to be an *infeasible solution*.
- Finally, if $b^2 - 4ac > 0$, then $x_{1,2}$ are real, the path segment intersects with the obstacle, and the path is an *infeasible solution*.

These three cases are analysed in Example (2).

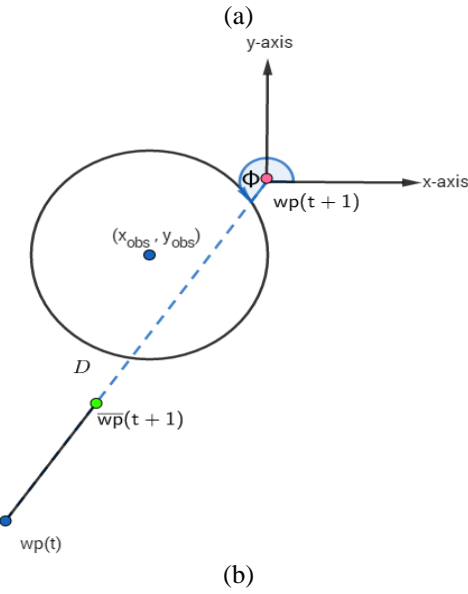
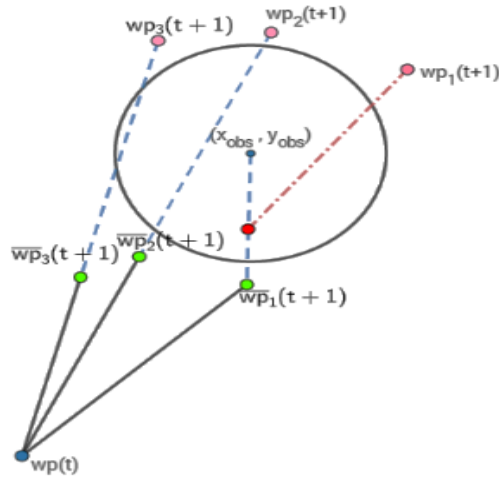


Fig. 6. Infeasible Path: The line segment passes through the obstacle.

Example (2): Suppose $obs_{pos} = (3, 3)$, $r_{obs} = 1$
Case 1: $wp_1(t) = (1, 2)$, $wp_1(t+1) = (3.5, 4.5)$
Case 2: $wp_2(t) = (1, 3)$, $wp_2(t+1) = (4, 5)$
Case 3: $wp_3(t) = (1, 4)$, $wp_3(t+1) = (5, 4)$
Check if these lines intersect with the obstacle or not.

Solution:

Case 1: Equation of the 1st line

$$\frac{y_2 - y_1}{x_2 - x_1} = \frac{y - y_1}{x - x_1} \Rightarrow \frac{4.5 - 2}{3.5 - 1} = \frac{y - 2}{x - 1}$$

$$\therefore \frac{y-2}{x-1} = 1 \Rightarrow y = x + 1 \quad (\text{Line equation})$$

Substituting this equation in the following circle equation that represents the obstacle,

$$(x - 3)^2 + (y - 3)^2 = 1^2 \quad (\text{circle equation})$$

yields

$$(x - 3)^2 + (x - 2)^2 = 1^2$$

$$x^2 - 5x + 6 = 0$$

Solving for x ,

$$x_1 = 3 \rightarrow y_1 = 4, \text{ intersection point 1 } (3, 4)$$

$$x_2 = 2 \rightarrow y_1 = 3, \text{ intersection point 2 } (2, 3)$$

$$b^2 - 4ac = (-5)^2 - (4 \times 1 \times 6) = 1 > 0$$

As the roots of the above equation are real numbers and the quadratic term $(b^2 - 4ac) > 0$, the line intersects the obstacle at two points.

Case 2: equation of the 2nd line,

$$\frac{y_2 - y_1}{x_2 - x_1} = \frac{y - y_1}{x - x_1}$$

$$\frac{5 - 3}{4 - 1} = \frac{y - 3}{x - 1}$$

$$\frac{y - 3}{x - 1} = 0.667$$

$$y = 0.667x + 2.33$$

$$(x - 3)^2 + (y - 3)^2 = 1^2$$

$$(x - 3)^2 + (y - 3)^2 = 1^2$$

Substituting the line equation into the circle equation, yields

$$(x - 3)^2 + (0.667x - 0.667)^2 = 1^2$$

$$1.4448x^2 - 6.8897x + 8.4448 = 0$$

Solving for x :

$$x_1 = 2.3 + 0.4i$$

$$x_2 = 2.3 - 0.4i$$

$b^2 - 4ac = 6.8897^2 - (4 \times 1.4448 \times 8.4448) = -1.3362$
As the roots of equation are complex numbers and quadratic term $(b^2 - 4ac) < 0$, the line does not intersect the obstacle.

Case 3: equation of line (3):

$$\frac{y_2 - y_1}{x_2 - x_1} = \frac{y - y_1}{x - x_1}$$

$$\frac{4 - 4}{5 - 1} = \frac{y - 4}{x - 1} \Rightarrow \frac{y - 4}{x - 1} = 0$$

$$y - 4 = 0 \Rightarrow y = 4$$

Substituting this equation in the following circle equation of the obstacle,

$$(x - 3)^2 + (y - 3)^2 = 1^2 \quad (\text{circle equation})$$

$$(x - 3)^2 + (4 - 3)^2 = 1^2$$

$$x^2 - 6x + 9 = 0$$

$$(x - 3)^2 + (4 - 3)^2 = 1^2$$

$$x^2 - 6x + 9 = 0$$

Solving for x , leads to $x_{1,2} = 3 \rightarrow y = 4$; one solution means one intersection point, since

$$b^2 - 4ac = (-6)^2 - (4 \times 1 \times 9) = 0$$

As the equation has one solution with quadratic term $(b^2 - 4ac) = 0$, the line is tangential to the obstacle

The solutions are updated by ousting the candidate solutions outside the region of the obstacle according to the following suggested rules (seen as green points in Fig. 6 (a)):

$$\bar{x}_{wp_j(t)} = x_{wp_j(t)} + (\delta * D) \times \cos \phi_j \quad (24)$$

$$\bar{y}_{wp_j(t)} = y_{wp_j(t)} + (\delta * D) \times \sin \phi_j \quad (25)$$

where δ is a design parameter and $\delta \in [0, 1]$, in our work it is chosen to be 0.6, and D is the distance between two consecutive points $wp_j(t+1)$ and $wp_j(t)$, ϕ_j as defined in Fig. 6 (b). The proposed rule is demonstrated in Example (3).

Example 3: Suppose that the obstacle position $obs_{pos} = (3, 3)$, radius of obstacle $r_{obs} = 1$, and candidate point suggested by hybrid PSO-MFB Algorithm is $wp(t+1) = (4, 4)$, and the previous way point $wp(t) = (1, 1)$.

Solution: Calculate the distance between $wp(t+1)$ & $wp(t)$, and assume $\delta = 0.6$

$$D = \sqrt{(x_{wp(t+1)} - x_{wp(t)})^2 + (y_{wp(t+1)} - y_{wp(t)})^2}$$

$$D = \sqrt{(4-1)^2 + (4-1)^2} = 4.242$$

$$\phi = 180 + \tan^{-1} \frac{y_{wp} - y_{pwp}}{x_{wp} - x_{pwp}}$$

$$\phi = 180 + \tan^{-1} \frac{4-1}{4-1} = 180^\circ + 45^\circ$$

Using Equations (20) and (21),

$$\bar{x}_{wp_j(t+1)} = x_{wp(t+1)} + 0.6 \times D \times \cos \phi = 2.2$$

$$\bar{y}_{wp_j(t+1)} = y_{wp(t+1)} + 0.6 \times D \times \sin \phi = 2.2$$

5.3. Obstacle detection and Avoidance (ODA)

In the previous section, the infeasible candidate solutions that might be generated by the proposed hybrid PSO-MFB algorithm and the proposed methods to convert them into feasible ones using the *LS* technique were discussed. In addition, when a moving obstacle gets closer to the mobile robot while the latter follows the feasible path generated by the proposed hybrid PSO-MFB algorithm, or the mobile robot itself gets closer to a static obstacle, it must instantly react to avoid this obstacle, or a collision will occur. In this section, the sensors deployment and a proposed method for sensing obstacles to achieve obstacle detection is thus presented, and a proposed method for avoiding these obstacles called the *gap vector method* is discussed.

5.3.1. Obstacle detection (OD) Procedure

Sensing is accomplished by attaching twelve virtual sensors around the mobile robot. These are separated equally, with each sensor covers an angle range of 30° and having a certain value of *Sensing Range* (SR), as shown in Fig. 7. In our design, it is taken as $SR = 0.8$ m.

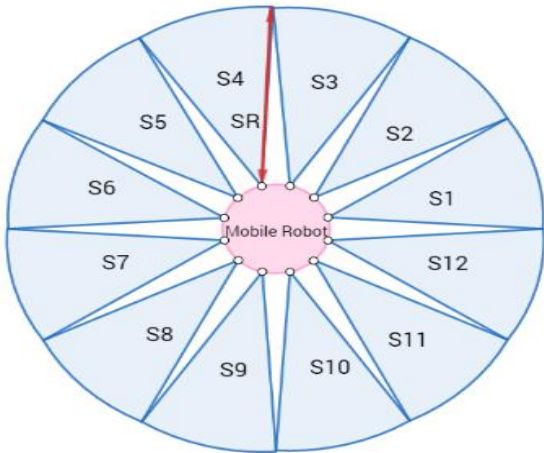


Fig.7. the layout of the mobile robot sensors.

The obstacles are detected using a *Sensory Vector* (V_s) with length equal to the number of deployed sensors:

$$V_s = [a(1) \quad \dots \quad a(i) \quad \dots \quad a(12)]$$

where $a(i)$, $i \in \{1, 2, \dots, 12\}$ are variables with binary values, and V_s reflects the status of an obstacle extant in an angle

range S_i , $i \in \{1, 2, \dots, 12\}$. For example, with $a(1) = a(2) = a(7) = \text{logic "1"}$, this indicates that obstacles are detected inside *SR* and in the angle range S_1 , S_2 , and S_7 respectively, while a logic "0" in a certain $a(i)$ s of V_s represents a free space in the corresponding angle ranges S_i s. To find V_s , for each obstacle located inside *SR* in a certain angle range, say S_i , draw the tangent lines to the expanded obstacle (red circle in Fig. 8) to intersect at the mobile robot A , $MR_{pos} = (x_{MR}, y_{MR})$. See Fig. 8.

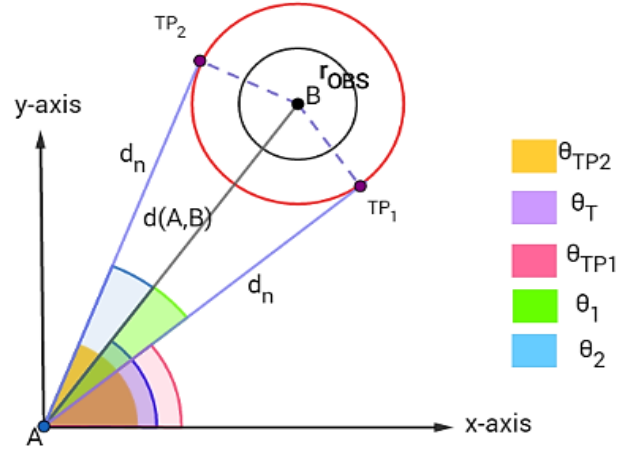


Fig.8. Angle between mobile robot and the obstacle.

Suppose that the distance between the mobile robot A with position $MR_{pos} = (x_{MR}, y_{MR})$ and the centre of the obstacle B with position $obsB_{pos} = (x_{obsB}, y_{obsB})$ is Euclidean distance $d(MR_{pos}, obsB_{pos})$, or simply d as given by (1). Compute angles θ_1 and θ_2 between the hypotenuse d and the tangent lines of the obstacle B extant in a certain S_i . Given $MR_{pos} = (x_{MR}, y_{MR})$ and $obsB_{pos} = (x_{obsB}, y_{obsB})$,

θ_T , which describes the angle between the mobile robot A and the obstacle B , can be easily found. From the basic geometry of triangles

$$\because r_{obs} \perp d_n \quad (\text{Property of Tangents})$$

$$\therefore d^2 = d_n^2 + r_{obs}^2 \quad (\text{Pythagoras theorem})$$

$$\theta_1 = \theta_2 = \sin^{-1} \frac{r_{obs}}{d} \quad (26)$$

$$\theta_{Tp1} = \theta_T - \theta_1 \quad (27)$$

$$\theta_{Tp2} = \theta_T + \theta_1 \quad (28)$$

Based on the above analysis, V_s is found by setting the values of $a(i)$ s, $i \in \{1, 2, \dots, 12\}$ in the V_s to logic "1" if the corresponding angle range S_i is occupied by static and/or dynamic obstacles. This is realized when the angle difference $\theta_{Tp2} - \theta_{Tp1}$ for each obstacle lies in the angle range S_i s. An example for the obstacle detection procedure using mobile robot path planning is depicted in Fig. 9; in this case,

$$V_s = [1 \ 1 \ 0 \ 0 \ 0 \ 0 \ 1 \ 1 \ 1 \ 0 \ 0 \ 0]$$

The obstacles $obs1$, $obs4$, and $obs3$ lie inside *SR*, and $obs1$ has an angle difference of $\theta_{Tp2} - \theta_{Tp1}$ that lies in the angle range ranges S_1 and S_2 , $obs3$ has its angle difference which lies in the angle ranges S_8 and S_9 . While $obs4$ has its own angle difference inside S_7 only.

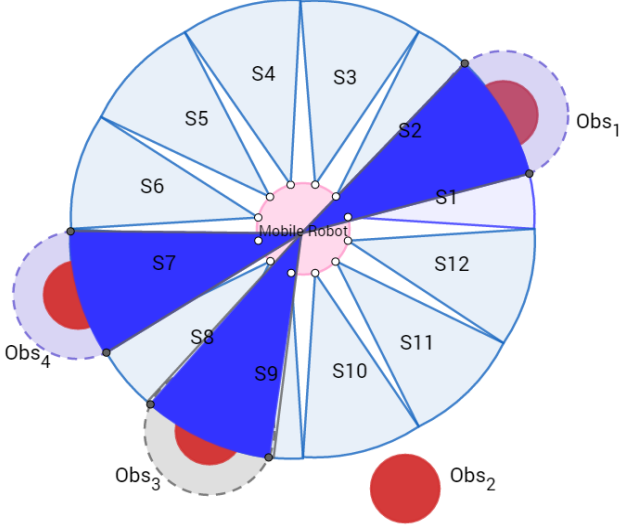


Fig. 9. Obstacle detection of mobile robot.

5.3.2. Obstacle Avoidance (OA) Algorithm

Obstacles avoidance is achieved by using a *gap vector* (V_g) concept, which is a binary vector where logic “1” represents an occupancy *gap* and logic “0” represents a *free gap*. The length of the gap vector V_g is equal to the length of V_s . The mobile robot chooses the gap that gives the shortest path moving towards GP . This V_g can be derived from the sensing vector V_s as follows: each consecutive zero in V_s represents a free gap (i.e., logic 0 in V_g); otherwise it is an occupied gap (i.e., logic 1 in V_g). This process is equivalent to an OR gate, as shown in Table 1.

Table 1 Gap Vector Construction

$V_s(i)$	$V_s(i+1)$	$V_g(i) = V_s(i) \vee V_s(i+1)$
0	0	0
0	1	1
1	0	1
1	1	1

where i is the sensor index. From the previous example (see Fig. 12), the above procedure yields:

$$V_s = [1 \ 1 \ 0 \ 0 \ 0 \ 1 \ 1 \ 1 \ 0 \ 0 \ 0]$$

$$V_g = [1 \ 1 \ 0 \ 0 \ 0 \ 1 \ 1 \ 1 \ 0 \ 0 \ 1]$$

After constructing V_g , several *free gaps* (permissible suggested mobile robot positions) are produced (see Fig. 10). The angle of each available free gap ψ_i is simply $\psi_j = j * 30$, where j is the index of the “0” in V_g . The next step is to determine the next position for the mobile robot (best free gap g_i in V_g), through which the mobile robot will evade the obstacles and continue moving toward GP using **Algorithm 1**. **Algorithm 2** describes the OA steps with details.

Fig. 10 offers an illustrative example. There are five available gaps in V_g , labelled g_3 , g_4 , g_5 , g_{10} , and g_{11} . Assume that all following positions and radii are in meters and that $MR_{Pos} = (3, 3)$, $obs1_{Pos} = (3.71, 3.41)$, $obs3_{Pos} = (2.31, 2.75)$, $obs4_{Pos} = (2.34, 2.76)$, $GP_{Pos} = (10, 10)$, $SR =$

Algorithm 2: Obstacle Avoidance (OA)

Step 1: Finding the distance between mobile robot and each obstacle within SR .

for $i=1:m$
 $d_i = d(MR_{Pos}, obs_i_{Pos})$
end

where $MR_{Pos} = (x_{MR}, y_{MR})$, $obs_i_{Pos} = (x_{obs_i}, y_{obs_i})$, m is the number of obstacles existing within SR .

The shortest distance (d_{sh}) is given as,

$$d_{sh} = \min(d_1, \dots, d_m)$$

Given r_{MR} , r_{OBS} , and SR ,

$$c = r_{MR} + r_{OBS} + SR;$$

j = index of the “zeros” in V_g

Step 4: Calculate the new allowable mobile robot positions, $g_{iPos} = (x_{gi}, y_{gi})$

for $i = j$

If ($d_{sh} < \frac{c}{2}$) **then**

$$x_{gi} = x_{MR} + 1.5 \times d_{sh} \times \cos \psi_i$$

$$y_{gi} = y_{MR} + 1.5 \times d_{sh} \times \sin \psi_i$$

Else

$$x_{gi} = x_{MR} + d_{sh} \times \cos \psi_i$$

$$y_{gi} = y_{MR} + d_{sh} \times \sin \psi_i$$

$d_{gi} = d(g_{iPos}, GP_{Pos})$ using (1), $g_{iPos} = (x_{gi}, y_{gi})$ and $GP_{Pos} = (x_{GP}, y_{GP})$

$j \leftarrow \text{new } j$

end

Step4: The best allowable position $g_{jPos} = (x_{gj}, y_{gj})$ is chosen by OA that has the smallest $d(g_{jPos}, GP_{Pos})$.

0.8, and $r_{MR} = r_{OBS} = 0.3$. The Euclidean distance between the mobile robot and each obstacle can be calculated as $d(MR_{Pos}, obs1) = 0.82$, $d(MR_{Pos}, obs3) = 0.73$, and $d(MR_{Pos}, obs4) = 0.7$. Therefore, $d_{sh} = 0.7$. It is obvious that all Euclidean distances between the mobile robot and the obstacles are larger than or equal to $\frac{c}{2}$. Specifically, $d_{sh} \geq \frac{c}{2}$ where $c = 0.3 + 0.3 + 0.8 = 1.4$. Thus, the new allowable mobile robot positions at the available free gaps can be calculated according to **Algorithm 2**; these are listed in Table (2).

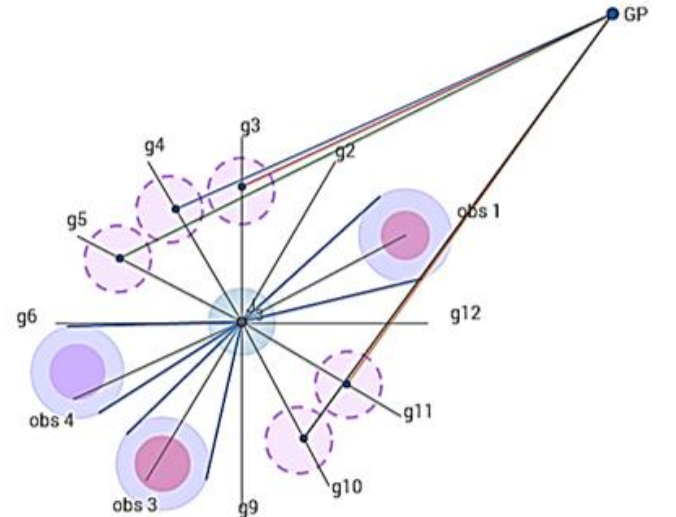


Fig. 10. Available free gaps.

Table 2 Calculations of the allowable mobile robot positions

Thus, the new allowable mobile robot position $MR_New_{Pos} = (x_{MR_New}, y_{MR_New})$ will be at $g3_{Pos} = (x_{g3}, y_{g3})$ and is given as

The mobile robot will evade the obstacles through gap $g3$, since this has shortest distance with GP, $dg3=9.4175$ m, as in Fig 10.

Algorithm 3: Path Planning Algorithm- Static and Dynamic Environments

6. Simulation Results

velocities, and directions of the dynamic obstacles are listed in Tables (4) and (5).

Table 4 Settings for the linear moving obstacles

Obstacle no.	Center	Radius(r_{OBS})	v_{obs} (m/s)	ϕ_{obs} (deg)
1	(7.5,2.1)	0.3	0.16	70°
2	(5.1,8.3)	0.3	0.13	0°

Table 5 Settings for the circular moving obstacles

Obstacle no.	Initial Position	Circle Centre (x_c, y_c)	Circle Radius (r_c)
3	(6,5)	(5, 5)	1
4	(4,5)	(5, 5)	1
5	(5,7.5)	(5, 5)	2.5
6	(5,2.5)	(5, 5)	2.5

The mobile robot navigates from its *SP* toward its *GP* using the proposed **Algorithm 3** as shown in Fig.12 (a) until it encounters an obstacle within its sensing region as depicted in Fig. 12 (b-e). At that time, the mobile robot triggers **Algorithm 2** to evade the obstacles and change its original path, using the proposed new collision-free path toward *GP*. The mobile robot continues its motion using **Algorithm 3** until it reaches *GP*. The best collision-free path obtained was 13.6696 m, as shown in Fig. 12(f).

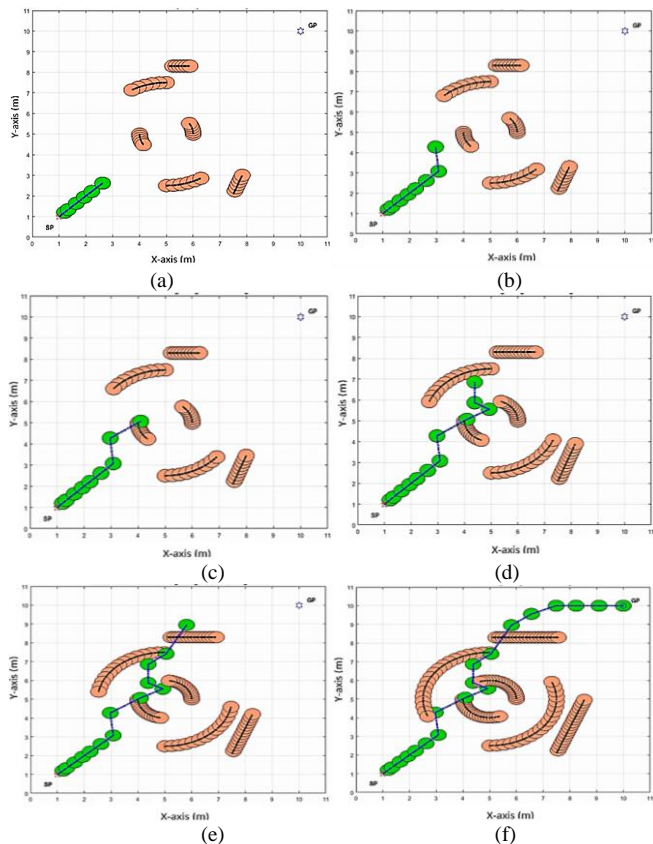


Fig. 12 The best path achieved with **Algorithm 3** for the above dynamic environment.

6.3. Comparison with Other Path Planning Algorithms

In this subsection, the performance of the proposed path planning algorithm using a hybrid PSO-MFB algorithm is compared with the works of [34–37]. The first case-study involved an environment also used in these works, which consists of four static obstacles. The optimisation techniques used to obtain the best path were the Direct Artificial Bee Colony (DABC) and Minimum Angle Artificial Bee Colony (MAABC) algorithms in [34, 35], while the work in [36] included GA and Bacterial Colony (BC) algorithms. The proposed Hybrid PSO-MFB algorithm was applied on the same environment as shown in Fig. 13.

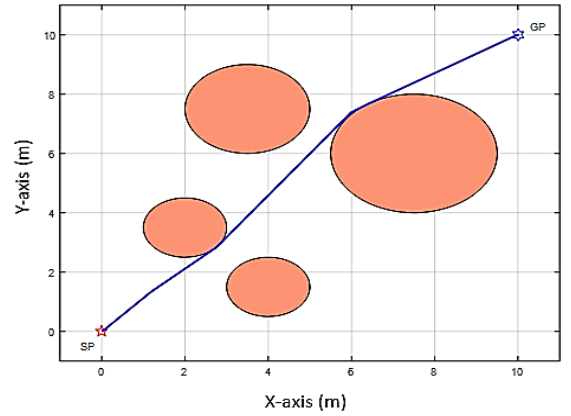


Fig. 13. The best path achieved using **Algorithm 3**.

The best path obtained using the proposed Hybrid PSO-MFB Algorithm was 14.3255 m, compared with 14.3625 m using DABC, 14.3371 m using MAABC, 14.5095 m using GA, and 14.3802 m using BC. The comparison with these works is illustrated in Table (6). It is worth mentioning that the environment size in [36] was 100m x 100m, and that this environment was scaled to 10m x 10m by dividing the results of GA and BC algorithms by a factor of 10 to make a fair comparison between the proposed PSO-MFB algorithm and the GA and BC ones.

Table 6 Comparison Results for the first case study with ten experiments

Optimization Technique	Max. Fitness	Min. Fitness	Mean Fitness	Standard deviation
Hybrid PSO-MFB	0.06980	0.06968	0.06977	0.0305
DABC	0.06962	0.06859	0.06934	0.0002
MAABC	0.06974	0.06865	0.06934	0.0079
GA	0.06892	0.06448	0.06778	0.0148
BC	0.06954	0.06908	0.06937	0.0014

Based on the above results, it is obvious that the Hybrid PSO-MFB algorithm outperforms the other optimisation techniques listed in Table (6). The last column in Table (6) is the standard deviation for each algorithm used in the comparison; this is a measure that tests the deviation of the results from different experiments executed under the same algorithm. Even with the large value of standard deviation of 0.0305 for the proposed hybrid PSO-MFB algorithm, this algorithm provided the best path,

which can be verified by the values of the mean, minimum, and maximum fitness values.

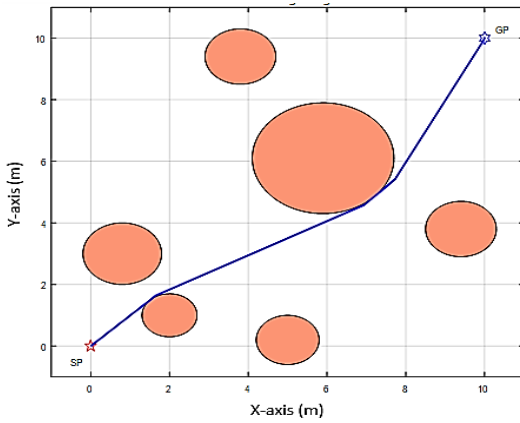


Fig. 14. The best path obtained using Algorithm 3.

The environment in [37], which involved six static obstacles, was used in the second case study for comparison. The optimisation technique used to obtain the shortest path was a standard ABC in [37], and DACB, and MAAB in [39 and 40]. The proposed Hybrid PSO-MFB algorithm was applied to the same environment, as shown in Fig. 14. The best path obtained using the proposed Hybrid PSO-MFB algorithm was 14.6384 m, compared to 14.7422 m and 14.7163 m using the DABC, MAABC algorithms, respectively. The best path using the ABC algorithm in [37] was 14.8821 m (after scaling by 10). The comparison results show that the proposed Hybrid PSO-MFB Algorithm outperforms ABC, DABC, and MAABC optimisation algorithms in terms of finding the shortest distance.

7. Conclusions

This paper proposed a path planning algorithm for mobile robots using a Hybrid PSO-MFB swarm optimisation algorithm integrated with Local Search (LS) and obstacle detection and avoidance (ODA) strategies. The size of the mobile robot was taken into account by enlarging the size of the obstacles in the free-space environment. The algorithm was tested in static and dynamic environments with different scenarios to minimise a multi-objective measure of path length and minimum angles. In the context of the simulation results, it can be concluded that the proposed hybrid PSO-MFB algorithm proved its efficacy in avoiding static and dynamic obstacles in a simple manner and reduced time. The simulation results demonstrated that the proposed path planning algorithm offers significant advances over current state-of-the-art options. In future work, consideration of the H/W implementation of the proposed Hybrid PSO-MFB algorithm-based path planning on real mobile platform should be made. Another possible future direction is implementing the proposed path planning algorithm in a dynamic environment with a moving goal.

References

- 1 Tzou, J.H., Su, K.L.: 'The development of the restaurant service mobile robot with a laser positioning system' *Proc. 27th Chinese Control Conf. CCC*, 2008, pp. 662–666.
- 2 Tzafestas, S.G.: 'Introduction to Mobile Robot Control' (Elsevier, 2014)
- 3 Garg, V., Tiwari, R.: 'A Chronological review of the approaches used for Multi Robot Navigation' *Int. Conf. Soft Comput. Tech. Eng. Technol.*, 2016, pp. 1–8.
- 4 Keil, J.M.: 'Decomposing a Polygon into Simpler Components' *SIAM J. Comput.*, 1985, **14**, (4), pp. 799–817.
- 5 Mohanty, P., Parhi, D.: 'Controlling the Motion of an Autonomous Mobile Robot Using Various Techniques: a Review' *J. Adv. Mech. Eng.*, 2013, pp. 24–39.
- 6 Khatib, O.: 'Real-Time Obstacle Avoidance for Manipulators and Mobile Robots.' *Int. J. Rob. Res.*, 1986, **5**, (1), pp. 90–98.
- 7 Mac, T.T., Copot, C., Tran, D.T., De Keyser, R.: 'Heuristic approaches in robot path planning: A survey' *Rob. Auton. Syst.*, 2016, **86**, pp. 13–28.
- 8 Deepak, B.B.V.L., Parhi, D.R., Raju, B.M.V.A.: 'Advance Particle Swarm Optimization-Based Navigational Controller For Mobile Robot' *Arab. J. Sci. Eng.*, 2014, **39**, (8), pp. 6477–6487.
- 9 Nasrollahy, A.Z., Javadi, H.H.S.: 'Using Particle Swarm Optimization for Robot Path Planning in Dynamic Environments with Moving Obstacles and Target' *2009 Third UKSim Eur. Symp. Comput. Model. Simul.*, 2009, (3), pp. 60–65.
- 10 Mohanty, P.K., Parhi, D.R.: 'Cuckoo search algorithm for the mobile robot navigation', in 'In International Conference on Swarm, Evolutionary, and Memetic Computing' (2013), pp. 527–536
- 11 Liang, X., Li, L., Wu, J., Chen, H.: 'Mobile robot path planning based on adaptive bacterial foraging algorithm' *J. Cent. South Univ.*, 2013, **20**, (12), pp. 3391–3400.
- 12 Das, P.K., Pradhan, S.K., Patro, S.N., Balabantaray, B.K.: 'Artificial Immune System Based Path Planning of Mobile Robot' *Soft Comput. Tech. Vis. Sci.*, 2012, **395**, pp. 195–207.
- 13 Dao, T.K., Pan, T.S., Pan, J.S.: 'A multi-objective optimal mobile robot path planning based on whale optimization algorithm', in 'IEEE 13th International Conference on Signal Processing (ICSP)', Chengdu, China, November 2016, pp. 337–342
- 14 Samadi, M., Othman, M.F.: 'Global Path Planning for Autonomous Mobile Robot Using Genetic Algorithm', in 'International IEEE Conference on Signal-Image Technology & Internet-Based

- Systems', Marrakesh, Morocco, November 2009 pp. 726–730
- 15 Huang, H.-C., Tsai, C.-C., Lin, S.-C.: 'SoPC-based parallel elite genetic algorithm for global path planning of an autonomous omnidirectional mobile robot', in 'IEEE International Conference on Systems, Man and Cybernetics', San Antonio, TX, USA, October 2009, pp. 2028–2033
 - 16 Kang, B.-Y., Lee, J., Kim, D.-W.: 'Fast genetic algorithm for robot path planning' *Electron. Lett.*, 2013, **49**, (23), pp. 1449–1451.
 - 17 Yang, S.X., Meng, M.: 'An efficient neural network approach to dynamic robot motion planning.' *Neural networks*., 2000, **13**, (2), pp. 143–148.
 - 18 Parhi, D.R., Singh, M.K.: 'Real-time navigational control of mobile robots using an artificial neural network' *Proc. Inst. Mech. Eng. Part C J. Mech. Eng. Sci.*, 2009, **223**, (7), pp. 1713–1725.
 - 19 Singh, M.K., Parhi, D.R.: 'Path optimisation of a mobile robot using an artificial neural network controller' *Int. J. Syst. Sci.*, 2011, **42**, (1), pp. 107–120.
 - 20 Wang, X., Hou, Z., Lv, F., Tan, M., Wang, Y.: 'A Target-Reaching Controller for Mobile Robots Using Spiking Neural Networks', in 'Proc. 19th Int. Conf. Neural Inf. Process' (Springer-Verlag Berlin, 2012), pp. 652–659
 - 21 Davis, Divya, and P.S.: 'Implementation of fuzzy-based robotic path planning', in 'Proceedings of the 2nd International Conference on Computer and Communication Technologies. Advances in Intelligent Systems and Computing', (2016), pp. 375–383
 - 22 Pandey, A., Parhi, D.R.: 'Optimum path planning of mobile robot in unknown static and dynamic environments using Fuzzy-Wind Driven Optimization algorithm' *Def. Technol.*, 2017, **13**, (1), pp. 47–58.
 - 23 Parhi, D.R., Mohanty, P.K.: 'IWO-based adaptive neuro-fuzzy controller for mobile robot navigation in cluttered environments' *Int. J. Adv. Manuf. Technol.*, 2016, **83**, (9–12), pp. 1607–1625.
 - 24 Castillo, O., Melin, P., Valdez, F., Martínez-Marroquín, R.: 'Optimization of Fuzzy Logic Controllers for Robotic Autonomous Systems with PSO and ACO' *Handb. Swarm Intell. Adapt. Learn. Optim.*, 2011, **8**, pp. 389–417.
 - 25 Teatro, T.A. V., Eklund, J.M., Milman, R.: 'Nonlinear Model Predictive Control for Omnidirectional Robot Motion Planning and Tracking With Avoidance of Moving Obstacles' *Can. J. Electr. Comput. Eng.*, 2014, **37**, (3), pp. 151–156.
 - 26 Chen, W.J., Jhong, B.G., Chen, M.Y.: 'Design of Path Planning and Obstacle Avoidance for a Wheeled Mobile Robot' *Int. J. Fuzzy Syst.*, 2016, **18**, (6), pp. 1080–1091.
 - 27 Bakdi, A., Hentout, A., Boutami, H., Maoudj, A., Hachour, O., Bouzouia, B.: 'Optimal path planning and execution for mobile robots using genetic algorithm and adaptive fuzzy-logic control' *Rob. Auton. Syst.*, 2017, **89**, pp. 95–109.
 - 28 Emam, M., Fakharian, A.: 'Path following of an omni-directional four-wheeled mobile robot', in '2016 Artificial Intelligence and Robotics, IRANOPEN 2016' (2016), pp. 36–41
 - 29 Kim, H., Kim, B.K.: 'Online minimum-energy trajectory planning and control on a straight-line path for three-wheeled omnidirectional mobile robots' *IEEE Trans. Ind. Electron.*, 2014, **61**, (9), pp. 4771–4779.
 - 30 Yang, J., Qu, Z., Wang, J., Conrad, K.: 'Comparison of optimal solutions to real-time path planning for a mobile vehicle' *IEEE Trans. Syst. Man, Cybern. Part A Systems Humans*, 2010, **40**, (4), pp. 721–731.
 - 31 Eberhart, R.C., Kennedy, J., Eberhart, R.C.: 'Particle swarm optimization' *Proc. IEEE Int. Conf. Neural Networks IV, pages*, 1995, **4**, pp. 1942–1948.
 - 32 Yang, X.-S., Cui, Z., Xiao, R., Gandomi, A.H., Karamanoglu, M.: 'Swarm Intelligence and Bio-Inspired Computation Theory and Applications' (2013)
 - 33 Ibraheem, Ibraheem Kasim, F.H.A.: 'Autonomous Mobile Robot Navigation and Obstacle Avoidance in Dynamic Environment using Modified Bat Swarm Optimization', in '1st International IEEE Conference on Recent Trends of Engineering Sciences and Sustainability', Baghdad, Iraq, May 2017, pp. 3631–3635
 - 34 Nizar Hadi Abbas, F.M.A.: 'Path Planning of an Autonomous Mobile Robot using Directed Artificial Bee Colony Algorithm' *Int. J. Comput. Appl.*, 2014, **96**, (11), pp. 11–16.
 - 35 Nizar Hadi Abbas, F.M.A.: 'Path Planning of an Autonomous Mobile Robot using Enhanced Bacterial Foraging Optimization Algorithm' *Al-Khwarizmi Eng. J.*, 2016, **12**, (4), pp. 26–35.
 - 36 Cezar A. Sierakowski, L. dos S.C.: 'Study Of Two Swarm Intelligence Techniques For Path Planning Of Mobile Robots', in 'Proceedings of 16th triennial world congress of the IFAC ', (2005), pp. 1–6
 - 37 Lin, J., Huang, L.: 'Chaotic bee swarm optimization algorithm for path planning of mobile robots', in 'Proceedings of the 10th WSEAS International Conference on Evolutionary Computing', Prague, Czech Republic, March, 2009, pp. 84–89.